

# A mathematical model and numeric method for contact analysis of rolling bearings

Shuting Li\*

Department of Mechanical, Electrical and Electronic Engineering,  
Interdisciplinary Faculty of Science and Engineering,  
Shimane University, Matsue, 690-8504, Japan

---

## Abstract

This paper deals with contact analysis of rolling bearings. A new mathematical model and numeric method are presented in this paper for the purpose of contact analysis of rolling bearings based on the principle of mathematical programming method. Three-dimensional (3D), finite element method (FEM) is introduced to calculate deformation influence coefficients and gaps of assumed pairs of contact points between the contact surfaces in the mathematical model. Special software is developed to realize numeric calculation procedures of the contact analysis. With the help of the developed software, loaded bearing contact analyses are conducted for a deep groove ball bearing and a cylindrical roller bearing. In the case of the ball bearing, it is found that calculated contact pressure on the ball surfaces is correct elliptical distribution (usually called contact ellipse). This result is more reasonable than the results obtained by commercial software SolidWorks and other researchers. In the case of the roller bearing, it is found that edge-loads (non-Hertz contact that cannot be analyzed with Hertz theory) on the roller surface are analyzed when the roller is not crowned. It is also found that the edge-loads disappear and contact pressure on the roller surface becomes uniform distribution when the roller is crowned with Johnson-Gohar curve. Since the most important features (contact ellipse and edge-loads) of the bearing contacts are analyzed successfully by the developed software and these results cannot be obtained simply by general methods, the mathematical model and numeric method presented in this paper are of practical meaning in engineering design and the developed software can be used as a tool for contact strength and rigidity calculations of the rolling bearings.

**Key Words** : Ball Bearing; Roller Bearing; Rolling Bearing; Contact Analysis; Finite Element Analysis (FEA).

## 1. Introduction

It is a very important thing for machine designers to evaluate contact strength, lifetime and radial rigidity of rolling bearings when they decide to use them. Unfortunately, it is still quite a difficult thing to evaluate the contact strength, lifetime and radial rigidity of the rolling bearings accurately in theory. This is because there have been some unsolved problems remained in strength and performance analyses of the rolling bearings, though it is quite a long history for machine designers to have been using rolling bearings in various kinds of machines.

In the case of ball bearings, usually, Hertz theory [1] is used to analyze contact pressure and radial rigidity of the ball bearings. But, since Hertz theory can consider only local deformation of contact areas of the ball bearings and the total structural deformation of the ball, outer ring and inner ring as well as bearing housings cannot be included, Hertz theory is not precise enough for contact analysis of the ball bearings when the structural deformation is very large.

---

\* Tel./fax: +81 0852 328908.

In the case of roller bearings, since edge-loads exist among contact surfaces, contact problem of the roller bearings does not belong to Hertz contact. It is a non-Hertz contact problem that cannot be solved by Hertz theory. In order to solve this problem, usually, an approximate model of using a roller contacting a surface of infinite length was suggested [2-4]. But, since this approximate model also cannot consider the effect of the structural deformation of the inner and outer rings, this model is also not precise enough for contact analysis of the roller bearings. Finally, FEM was suggested to do contact analysis of the roller bearings [2,5]. Indeed, FEM is a very practical method for engineering structural analysis and successful in many kinds of engineering calculations. But, unfortunately, it is not so successful in contact analysis of machines or machine elements for the available FEM. So, it is necessary to present a new method that can solve the contact analysis problem of machines or machine elements well.

So far, there have been many studies found on rolling bearings. Wang [6] studied on contact finite element simulation of the high angular contact thrust ball bearing. Qi [7] conducted contact analysis of deep groove ball bearings in multibody systems using theoretical method. Zhang [8] studied the relationship between stiffness and preload for an angular contact ball bearing using theoretical method. Casanova [9] studied the contribution of the deflection of tapered roller bearings to the misalignment of the pinion in a pinion-rack transmission. But the most important features (contact pressure distribution, edge-loads and crowning) for the bearing contacts were not discussed in these studies. Of course, it cannot be said that contact problem of the rolling bearings has been solved by these studies. Other studies were also found on dynamic analysis of the rolling bearings. Xu [10-12] studied the dynamic load calculation of deep groove ball bearing joints in planar multibody systems. Liu [13-14] studied vibration problem of a ball bearing system using a lumped spring-mass model. Singh [15] analyzed the contact forces and vibration response for a defective rolling element bearing using an explicit dynamics finite element model. Bovet [16] presented a modelling approach for predicting the internal dynamic behavior of ball bearings under high moment loads. Machado [17] also studied dynamic stress analysis of rolling bearings through proposing the discrete element method. In these researches, vibration analysis theories were used to investigate the vibration problem of the bearings used in machines. The static contact problems of the rolling bearings could not be investigated in these studies.

This paper tries to present a new numeric method that can solve the contact problem of the rolling bearings precisely. A new mathematical model is presented in this paper for contact analysis of the rolling bearings based on the principle of mathematical programming method at the first. Then, 3D, FEM is introduced in the mathematical model to calculate deformation influence coefficients and gaps of assumed pairs of contact points on contact surfaces. Special software is developed through long-time efforts. With the help of the developed software, contact analyses are conducted for a deep groove ball bearing and a cylindrical roller bearing respectively. In the case of the ball bearing, it is found that calculated contact pressure on the ball surfaces is correct elliptical distribution (usually called contact ellipse). This result is more reasonable than the results obtained by commercial software SolidWorks and other researchers. In the case of the roller bearing, it is found that edge-loads (non-Hertz contact that cannot be analyzed with Hertz theory) on the roller surface are analyzed when the roller is not crowned. It is also found that the edge-loads disappear and contact pressure on the roller surface becomes uniform distribution when the roller is crowned with Johnson-Gohar curve. Since the most important features (contact ellipse and edge-loads) of the bearing contacts are analyzed successfully by the developed software and these results cannot be obtained simply by general methods, the mathematical model and numeric method presented in this paper are of practical meaning in engineering

design and the developed software can be used as a useful tool for contact strength and rigidity calculations of the rolling bearings.

## 2. Bearings used as research objects

Structures and dimensions of the rolling bearings used as research objects are illustrated in Fig.1. In Fig.1, (a) and (b) are a deep groove ball bearing (type number 6332) and a cylindrical roller bearing (type number NU412) respectively. They are made by NTN, a Japanese bearing company [18]. Contact analyses are conducted for them using commercial software SolidWorks at the first, and then using the special software developed in this paper. Hertz theory is also used to calculate contact pressure and radial rigidity of the ball bearing in order to make a comparison with the special software.

Materials of the outer ring, rolling elements and inner ring are SUJ2 (Japanese material name). Young's modulus and Poisson's ratio of the material are 210GPa and 0.3. In the case of the roller bearing as shown in Fig. 1(b), since a cylindrical roller bearing is used as the research object, it is assumed that there is no axial load existing in the bearing. This means that the rollers do not contact with the cage of outer ring. So, the contact between the roller and the cage can be neglected in the contact analysis.

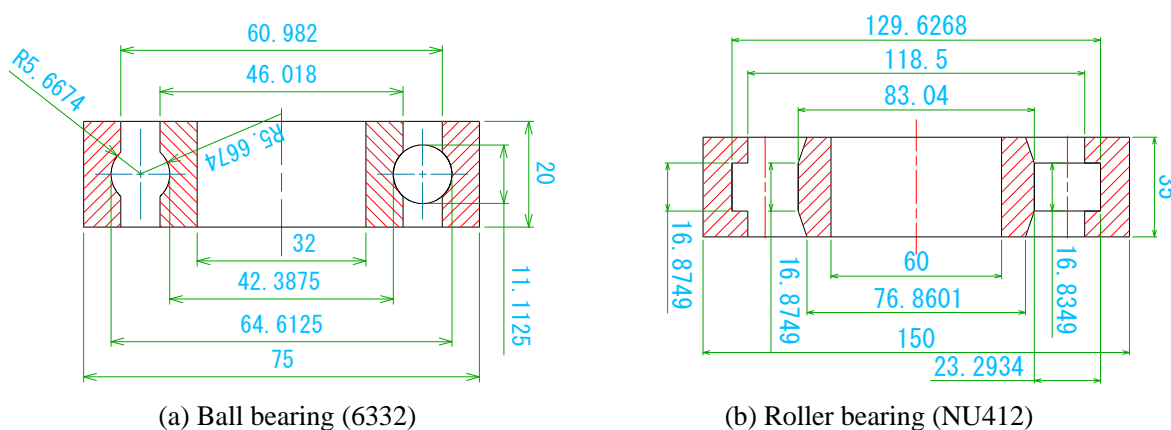


Fig. 1. The ball and roller bearings used as research objects

## 3. Problems of commercial software SolidWorks in contact analysis of bearings

As mentioned above, commercial software is successful in many kinds of engineering calculations, but it is not so successful in contact analysis of machines and machine elements. In order to explain this problem clearly, the commercial software SolidWorks is used here to conduct contact analysis of the ball and roller bearings given in Fig. 1. This is because SolidWorks software is mostly used in mechanical companies. Calculation results are introduced in the following.

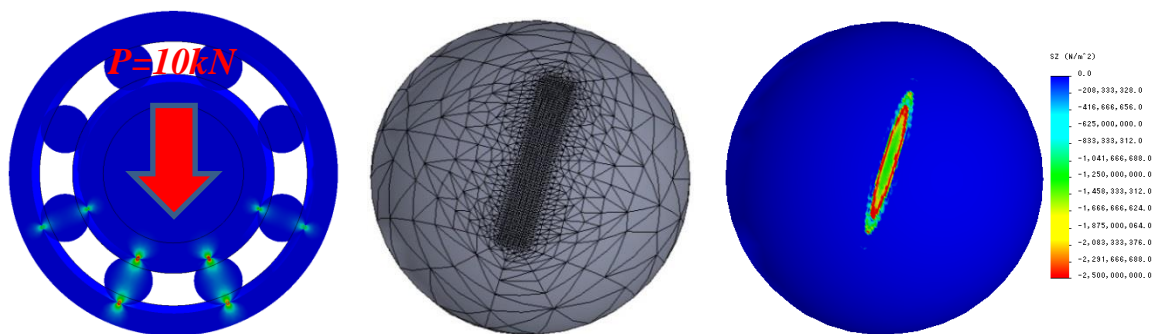
In SolidWorks, there is a function called "SolidWorks Simulation" that can be used to do engineering simulations. "SolidWorks Simulation" is originated from the famous software COSMOSWorks (the old name is SAP) [19]. In the software of COSMOSWorks, a function of contact analysis is also included. So, this paper uses this function to conduct contact analyses of the ball and roller bearings in Fig. 1. FEM models and some calculation results [20] are shown in Fig. 2 and 3. When the contact analyses are conducted, a radial load  $P$  is applied on the inside surfaces of the inner rings as shown in Fig. 2(a) and 3(a) through bearing shafts that are used to insert into

the central holes of the inner rings. The outside surfaces of the outer rings are fixed as the boundary conditions for FEA. The bearing shaft and the inner ring are unified as one elastic body in the FEA.

Calculation results of the ball bearing are given in Fig. 2. In Fig. 2, (a) is a contour map of calculated Von Mises stresses distributed on the central section that goes through the ball centre and is perpendicular to the bearing axis. Fig. 2(a) indicates that only four balls at the lower part of the bearing are in contact with the raceways of the inner and outer rings. Fig. 2(b) is FEM mesh-dividing pattern of the ball. As shown in Fig. 2(b), meshes of the contact areas on the ball surface are fine-divided in order to ensure high calculation accuracy. Of course, meshes of the contact areas on the raceways of the inner and outer rings are also fine-divided responsively. Fig. 2(c) is a contour map of calculated contact pressure distributed on the ball surface. From Fig. 2(c), it is found that the maximum contact pressure is not located at the centre of the contact ellipse. It is calculated to distribute along a closed elliptical curve illustrated in the red line in Fig. 2(c). It is also found that the maximum contact pressure is calculated to be about twice the value obtained by using Hertz theory. This means that the commercial software SolidWorks cannot conduct correct contact analysis of the ball bearings.

Calculation results of the roller bearing are given in Fig. 3. In Fig. 3, (a) is a contour map of calculated Von Mises stresses distributed on the central section going through the centre of the roller width and being perpendicular to the bearing axis. Fig. 3(a) indicates that only four rollers at the lower part of the bearing are in contact with raceways of the inner and outer rings. Fig. 3(b) is FEM mesh-dividing pattern of the roller. As shown in Fig. 3(b), meshes of the contact areas on the roller surface are fine-divided. Meshes of the contact areas on the raceways of the inner and outer rings are also fine-divided responsively. Fig. 3(c) is a contour map of calculated contact pressure distributed on the roller surface. From Fig. 3(c), it is found that contact pattern of the roller takes the shape of an oval (the roller is crowned longitudinally using Johnson-Gohar curve [21]). It is also found that the maximum contact pressure is not located at the centre of the contact ellipse. It is calculated to distribute along a closed elliptical curve illustrated in the red line in Fig. 3(c). This also means that the commercial software SolidWorks cannot conduct correct contact analysis of the roller bearings.

Per long-time experiences of the author on CAE simulation using the commercial software, it is found that not only SolidWorks, but also other commercial software has the same problem as SolidWorks that it cannot conduct precise contact analyses of machines or machine elements. In the next research, ANSYS, ADINA and ABAQUS shall be used to do contact analyses of the rolling bearings. The calculated results shall be compared with the ones obtained by the method in this paper.



(a) Von Mises stress distribution      (b) FEM mesh-dividing      (c) Contact pressure on the ball

Fig. 2. Calculation results of the ball bearing using SolidWorks (P=10kN)

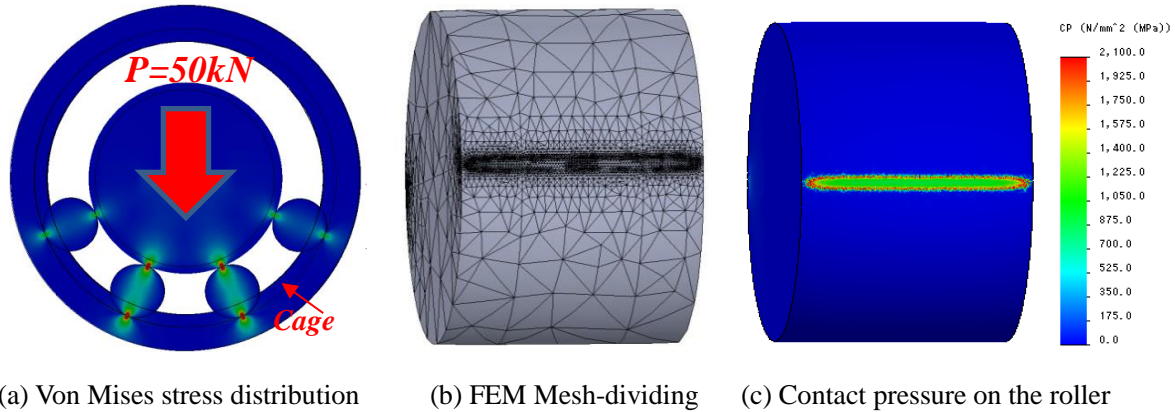


Fig. 3. Calculation results of the roller bearing using SolidWorks (P=50kN)

Guo and Parker [22] also conducted contact analyses for a deep groove ball bearing and a cylindrical roller bearing using special FEM software. Calculation results obtained by Guo and Parker are given in Fig. 4. In Fig. 4, (a) and (b) are contact load distribution on the ball and roller surfaces respectively. In Fig. 4(a), the well-known contact ellipse as shown in Fig. 2(c) cannot be found on contact area of the ball surface. In Fig. 4(b), the well-known edge-loads or contact ellipse as shown in Fig. 11 and Fig. 13 cannot be found on contact area of the roller surface. This means that calculation results in Figs. 4(a) and 4(b) have no features of contact pressure distribution of the ball and roller bearings. So, it can be said that quite rough results were obtained in Guo and Parker's research.

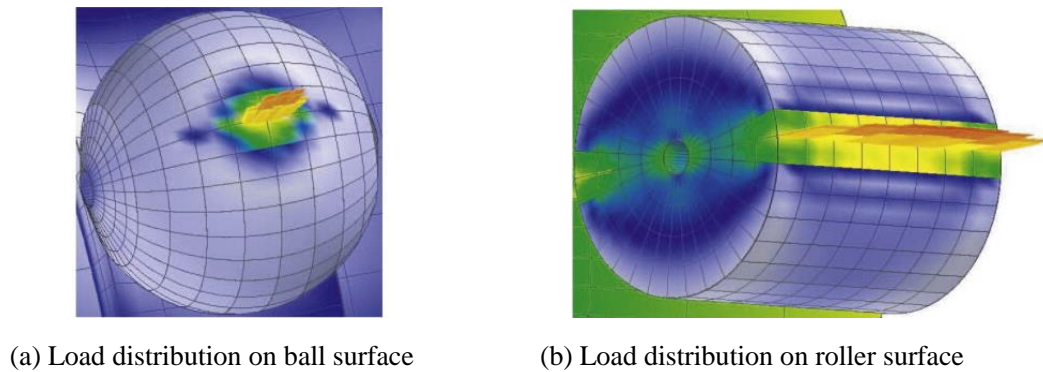
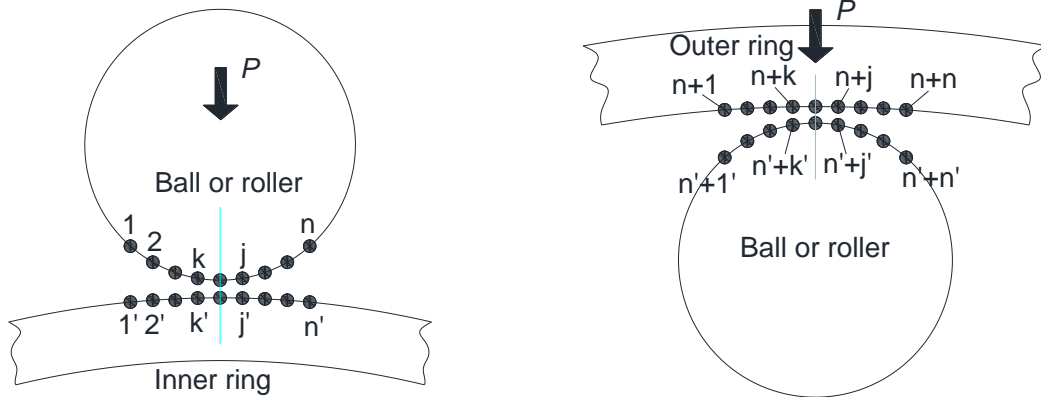


Fig. 4. Guo and Parker's results on bearing contact analysis [22]

Based on the results mentioned above, it is found that the well-known contact ellipse for the ball bearings and edge-loads or contact ellipse for the roller bearings cannot be calculated correctly. So, it can be understood that it is still a difficult thing at the present situation to conduct correct loaded bearing contact analysis using SolidWorks software and the special method introduced in the reference [22]. It is necessary to develop a new method that can conduct contact analysis of the bearings correctly. This paper tries to suggest a new mathematical model and numeric method for the contact analysis of rolling bearings.

## 4. A new mathematical model and numeric method for contact analysis of rolling bearings

### 4.1 Principle used for contact analysis of rolling bearings



(a) Contact of a ball or roller with the inner ring

(b) Contact of a ball or roller with the outer ring

Fig. 5. Mechanics models used for contact analysis of rolling bearings

Mechanics models used for contact analysis of rolling bearings are given in Fig. 5. In Fig. 5, (a) is used to stand for the contact problem of a ball or roller with the inner ring raceway and (b) is used to stand for the contact problem of the ball or roller with the outer ring raceway. It is assumed that an external load  $P$  (usually, equals to radial load of the bearings) is applied on the bearing in vertical direction as shown in Fig. 5. It is assumed that only elastic deformation occurred in the contact problems of the rolling bearings.

In Fig. 5(a), a lot of pairs of contact points, such as  $(1-1')$ ,  $(2-2')$ , ...,  $(j-j')$ , ...,  $(k-k')$  and  $(n-n')$ , are assumed on the contact surfaces of the ball (roller) and the inner ring raceway along the vertical direction. The points  $1, 2, \dots, j, \dots, k$  and  $n$  are assumed to be on the contact area of the ball (roller) surface. The points  $1', 2', \dots, j', \dots, k'$  and  $n'$  are assumed to be responsive points of the points  $1, 2, \dots, j, \dots, k$  and  $n$  on the contact area of the inner ring raceway. The common normal lines of these assumed pairs of contact points are parallel to the vertical direction and pass through the pairs of contact points. These pairs of contact points are possible enough to come into contact when the external load  $P$  is applied.

#### 4.1.1 Deformation compatibility relationship of the pairs of contact points

As shown in Fig. 5(a), for an optional (arbitrary) pair of contact points  $(k-k')$ ,  $F_k$  is used to denote contact force between the pair of contact points  $(k-k')$ . Direction of  $F_k$  is along its common normal line. Also,  $F_j$  is the contact force between the pair of contact points  $(j-j')$  along its common normal line. Gaps between the pairs  $(j-j')$ ,  $(k-k')$  and  $(n-n')$  are denoted as  $\varepsilon_j$ ,  $\varepsilon_k$  and  $\varepsilon_n$  respectively. The total relative deformation of the ball or roller relative to the inner ring along the load  $P$  is denoted as  $\delta_1$ . Elastic deformation of the pair  $(k-k')$  along the common normal line is denoted as  $\omega_k$  and  $\omega_{k'}$ , respectively. When the external load  $P$  is applied, if the pair  $(k-k')$  comes into contact, then  $(\omega_k + \omega_{k'} + \varepsilon_k)$ , the amount of deformation and gap of the pair  $(k-k')$ , shall be equal to the relative deformation  $\delta_1$ . On the other hand, if the pair  $(k-k')$  doesn't come into contact, then  $(\omega_k + \omega_{k'} + \varepsilon_k)$  shall be greater than  $\delta_1$ . These relationships are deformation compatibility relationships. They can be expressed with Eq. (1) and (2) in the following. Also, Eq. (1) and (2) can be summarized into Eq. (3). Eq. (3) is not only suitable for the optional pair  $(k-k')$ , but also suitable for all the pairs of contact points assumed on the contact surfaces. In Eq. (3),  $n$  is the total pair number of

the assumed contact points.

$$\omega_k + \omega_{k'} + \varepsilon_k - \delta_1 > 0 \quad (\text{Not contact}) \quad (1)$$

$$\omega_k + \omega_{k'} + \varepsilon_k - \delta_1 = 0 \quad (\text{Contact}) \quad (2)$$

$$\omega_k + \omega_{k'} + \varepsilon_k - \delta_1 \geq 0 \quad (k = 1, 2, \dots, n) \quad (3)$$

Since the elastic deformation  $\omega_k$  and  $\omega_{k'}$  can be expressed with deformation influence coefficients  $a_{kj}$  and  $a_{k'j'}$ , Eq. (4) and (5) can be obtained. If Eq. (4) and (5) are substituted into Eq. (3), then Eq. (6) can be obtained. Where,  $a_{kj}$  and  $a_{k'j'}$  are deformation influence coefficients of the pairs of contact points along their common normal lines.  $a_{kj}$  and  $a_{k'j'}$  can be calculated using 3D, FEM. The detailed procedures how to calculate  $a_{kj}$  and  $a_{k'j'}$  can be found in the reference [23-25].

$$\omega_k = \sum_{j=1}^n a_{kj} F_j \quad (4)$$

$$\omega_{k'} = \sum_{j=1}^n a_{k'j'} F_j \quad (5)$$

$$\sum_{j=1}^n [a_{kj} + a_{k'j'}] \times F_j + \varepsilon_k - \delta_1 \geq 0 \quad (k = 1, 2, \dots, n) \quad (6)$$

#### 4.1.2 Load equilibrium relationship of the pairs of contact points

Except for the deformation compatibility relationship as shown in Eq. (6), a load equilibrium relationship of the pairs of contact points also can be built as given in Eq. (7). Where,  $P$  is the external load applied on the bearing.

$$\sum_{k=1}^n F_k = P \quad (k = 1, 2, \dots, n) \quad (7)$$

In the case of the ball (roller) contacting the outer ring as illustrated in Fig. 5(b), the deformation compatibility relationship and load equilibrium relationship also can be built in the same way as given in Eq. (8) and (9) for the assumed pairs of contact points on the ball (roller) and outer ring raceway surfaces. Where,  $\delta_2$  is relative deformation of the ball (roller) relative to the outer ring along the direction of  $P$ .

$$\sum_{j=n+1}^{n+n} [a_{kj} + a_{k'j'}] \times F_j + \varepsilon_k - \delta_2 \geq 0 \quad (k = n + 1, \dots, n + n) \quad (8)$$

$$\sum_{k=n+1}^{n+n} F_k = P \quad (k = n + 1, \dots, n + n) \quad (9)$$

If adding Eq. (6) and Eq. (8) together, then Eq. (10) can be obtained. Also, if adding Eq. (7) and Eq. (9) together, then Eq. (11) can be obtained. Where,  $\delta = \delta_1 + \delta_2$  is the total relative deformation among the outer ring, ball (roller) and inner ring along the direction of  $P$ . If Eq. (10) is written into a matrix expression, then Eq. (12) can be obtained. Also, if Eq. (11) is written into a matrix form, then Eq. (13) can be obtained.

$$\sum_{j=1}^{2n} [a_{kj} + a_{k'j'}] \times F_j + \varepsilon_k - \delta \geq 0 \quad (k = 1, 2, \dots, 2n) \quad (10)$$

$$\sum_{k=1}^{2n} F_k = 2P \quad (k = 1, 2, \dots, 2n) \quad (11)$$

$$[S]\{F\} + \{\varepsilon\} - \delta\{e\} \geq \{0\} \quad (12)$$

Where,

$$[S] = \begin{bmatrix} [S1] & [0] \\ [0] & [S2] \end{bmatrix}$$

$$[S1] = [S_{kj}] = [a_{kj} + a_{k'j'}], k = 1, 2, 3, \dots, n; j = 1, 2, 3, \dots, n$$

$$[S2] = [S_{kj}] = [a_{kj} + a_{k'j'}], k = n + 1, n + 2, \dots, n + n; j = n + 1, n + 2, \dots, n + n$$

$$[0] = \begin{bmatrix} 0 & \dots & 0 \\ \vdots & \ddots & \vdots \\ 0 & \dots & 0 \end{bmatrix}$$

$$\{F\} = \{F_1, F_2, \dots, F_k, \dots, F_{n+n}\}^T$$

$$\{\varepsilon\} = \{\varepsilon_1, \varepsilon_2, \dots, \varepsilon_k, \dots, \varepsilon_{n+n}\}^T$$

$$\{e\} = \{1, 1, \dots, 1\}^T$$

$$\{0\} = \{0, 0, \dots, 0\}^T$$

$$\{e\}^T \{F\} = 2P \quad (13)$$

#### 4.2. A new mathematical model used for contact Analysis of the rolling bearings

A new mathematical model is built to solve the contact problem of bearings based on the principle of mathematical programming method [26-27] as follows.

Since Eq. (12) is an inequality equation that may be strictly positive or identically zero, it can be transformed into an equality equation if a variable  $\{Y\} = \{Y_1, Y_2, \dots, Y_k, \dots, Y_{2n}\}^T$  (consists of positive variables) is introduced in Eq. (12) and let  $[S]\{F\} + \{\varepsilon\} - \delta\{e\} = [I]\{Y\}$ , Where,  $[I]$  = a unit matrix of  $2n \times 2n$ . From this equation, then Eq. (14) can be obtained. Also, if change positions of the array and matrix in Eq. (14), then Eq. (15) can be obtained.

$$[S]\{F\} + \{\varepsilon\} - \delta\{e\} - [I]\{Y\} = \{0\} \quad (14)$$

$$-[S]\{F\} + \delta\{e\} + [I]\{Y\} = \{\varepsilon\} \quad (15)$$

Where,  $\{Y\} = \{Y_1, Y_2, \dots, Y_k, \dots, Y_{2n}\}^T$  (Slack variables);  $[I]$  = a unit matrix of  $2n \times 2n$ .

The positive variable  $\{Y\}$  is also called slack variable in the modified simplex method [26-27]. Now, two equality equations of Eq. (13) and (15) are available. According to the principle of the modified simplex method, the equality equations shall be used as constrain conditions in the mathematical model of the modified simplex method. So, Eq. (13) and (15) are used as constrain conditions since they are equality equations. The next task is to make an objective function  $Z$  that is necessary for the mathematical model of the modified simplex method.

According to the principle of the modified simplex method, in the case of a mathematical model without objective function, the objective function can be introduced artificially. That is to say, some positive variables  $X_{2n+1}, X_{2n+2}, \dots, X_{2n+2n}, X_{2n+2n+1}$  can be introduced and the objective function  $Z$  can be made through  $Z = X_{2n+1}, X_{2n+2}, \dots, X_{2n+2n}, X_{2n+2n+1}$ . These positive variables  $X_{2n+1}, X_{2n+2}, \dots, X_{2n+2n}, X_{2n+2n+1}$  are called artificial variables in the modified simplex method [26-27]. When the artificial variables are introduced, they must be also added to every constrain equation. Finally, the mathematical model used for contact analysis of the bearings is made as follows according to the principle of the modified simplex method.

### Mathematical model used for bearing contact analysis

#### Objective Function:

$$Z = X_{2n+1} + X_{2n+2} + \dots + X_{2n+2n} + X_{2n+2n+1} \quad (16)$$

#### Constraint Conditions:

$$-[S]\{F\} + \delta\{e\} + [I]\{Y\} + [I]\{Z'\} = \{\varepsilon\} \quad (17)$$

$$\{e\}^T\{F\} + X_{2n+2n+1} = 2P \quad (18)$$

Where,

$$\{Z'\} = \{X_{2n+1}, X_{2n+2}, \dots, X_{2n+2n}\}^T \text{ (Artificial variables)}$$

$$[S] = \begin{bmatrix} [S1] & [0] \\ [0] & [S2] \end{bmatrix} \quad (19)$$

$$[S1] = [S_{kj}], k = 1, 2, 3, \dots, n; j = 1, 2, 3, \dots, n$$

$$[S2] = [S_{kj}], k = n + 1, n + 2, \dots, n + n; j = n + 1, n + 2, \dots, n + n$$

$$[0] = \begin{bmatrix} 0 & \dots & 0 \\ \vdots & \ddots & \vdots \\ 0 & \dots & 0 \end{bmatrix} \quad (n \times n)$$

$$\{F\} = \{F_1, F_2, \dots, F_k, \dots, F_{2n}\}^T$$

$$\{Y\} = \{Y_1, Y_2, \dots, Y_k, \dots, Y_{2n}\}^T \text{ (Slack variable)}$$

$$\{\varepsilon\} = \{\varepsilon_1, \varepsilon_2, \dots, \varepsilon_k, \dots, \varepsilon_{2n}\}^T$$

$$\{e\} = \{1, 1, \dots, 1\}^T$$

$$F_k \geq 0, Y_k \geq 0, \varepsilon_k \geq 0, \delta \geq 0, k = 1, 2, \dots, 2n$$

$$X_{2n+m} \geq 0, m = 1, 2, \dots, 2n + 1$$

The above model consists of Eq. (16) to Eq. (18). This model is a mathematical model of optimization problem and it is called mathematical model simply in this paper. In the model, Eqs. (17) and (18) are used as constrain conditions in contact analysis of the bearings to identify which pair of contact points is in contact and which pair is not in contact when the external load  $P$  is applied. The contact force  $F_k$  and the total radial deformation  $\delta$  can be calculated by minimizing the objective function  $Z$  in Eq. (16) under the constrain conditions of Eqs. (17) and (18) using the modified simplex method [26-27].

Therefore, contact problem of bearings can be explained as looking for the contact force  $F_k$  ( $k = 1, 2, 3, \dots, 2n$ ) of the pairs of contact points that must satisfy Eqs. (13) and (15) under the conditions of knowing deformation influence coefficients  $a_{kj}$ ,  $a_{k'j'}$ , gaps  $\varepsilon_k$  and the external load  $P$  in advance.

#### 4.3 Software development

Software is developed to realize procedures of the bearing contact analysis. Firstly, 3D, FEM is used to calculate the deformation influence coefficients  $a_{kj}$ ,  $a_{k'j'}$ , that are necessary to form [S1] and [S2] in the matrix [S]. Special FEM software is developed using super-parametric hexahedron solid element, which has 8 nodes at the corner and 3 nodes inside the element [28]. This is because even if the meshes at the part contact areas are divided to be very narrow, the finite element analysis can converge and get good calculation precision.

FEM mesh-dividing patterns of the ball and roller bearings are given in Fig. 6 and 7 respectively. Fig. 6(a) and Fig. 7(a) are the FEM mesh-dividing patterns of the whole ball and roller bearings respectively. Fig. 6(b) and Fig. 7(b) are enlarged view of the FEM mesh-dividing patterns of ball and roller respectively. Before contact analyses of

the bearings are conducted, contact areas are defined (assumed) firstly on the surfaces of the outer ring, rolling elements and inner ring around the geometric contact point for the ball bearing and the geometric contact line for the roller bearing. Maybe, the assumed contact areas turn out to be very larger or very smaller than the real contact areas after the contact analyses are conducted. But, it is not a problem for the definition at the first. The size of contact areas can be changed by parameters in the developed software at the second time of contact analysis. So, if this change and contact analysis are repeated until a suitable contact area is found, the contact analysis can be ended. As shown in Fig. 6 and 7, meshes on the contact areas of the outer rings, ball (roller) and inner rings are fine-divided to ensure high calculation accuracy of FEA.

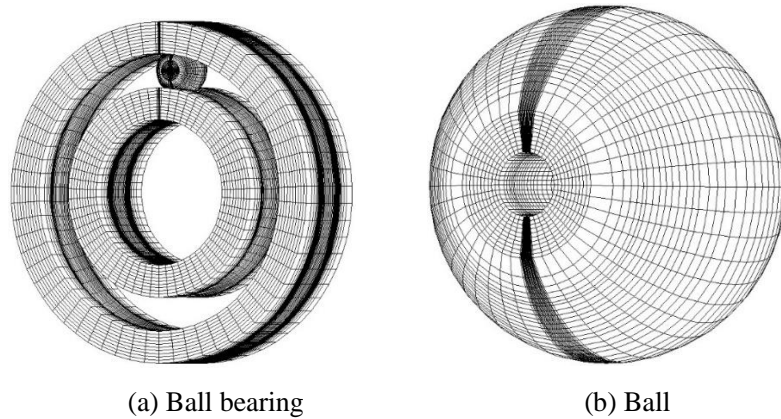


Fig. 6. Mesh-dividing patterns of the ball bearing

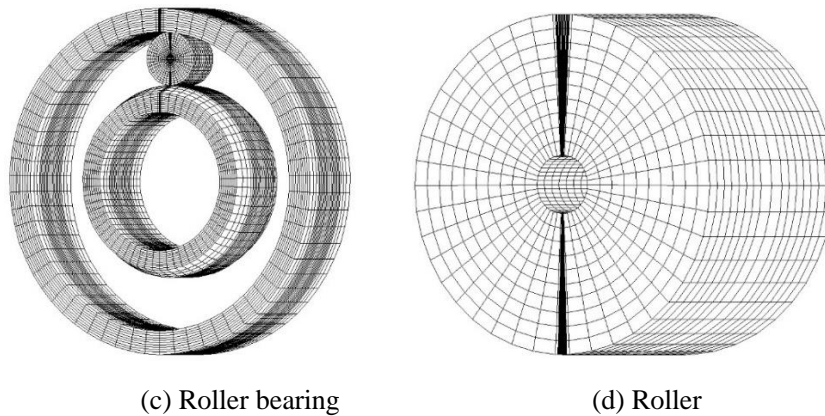


Fig. 7. Mesh-dividing patterns of the roller bearing

Software is developed to realize the procedures of the contact analysis after the deformation influence coefficients are available through FEA. Then, contact load  $\{F\}$  and the total radial deformation  $\delta$  can be calculated after the mathematical programming procedures are finished. Contact pressure distribution can be available after the contact load  $\{F\}$  is obtained through calculating contact load distributed on unit contact area. The radial rigidity  $K$  of bearings can also be obtained through this calculation  $K = P/\delta$ .

In order to have enough precision of the calculated contact pressure, number of the assumed contact points within the contact width should be greater than 10. The relationship between the assumed contact points and calculation precision was investigated in detail in the reference [23-25]. In this paper, the assumed contact points within the contact and in the axial direction are 21 and 41 respectively. This means that there are  $21 \times 41 = 861$  pairs of the assumed contact points made on the contact surfaces.

Flowchart used to develop the software is given in Fig. 8. The method used to realize the numeric calculation procedure as shown in Fig. 8 is called numeric method in this paper.

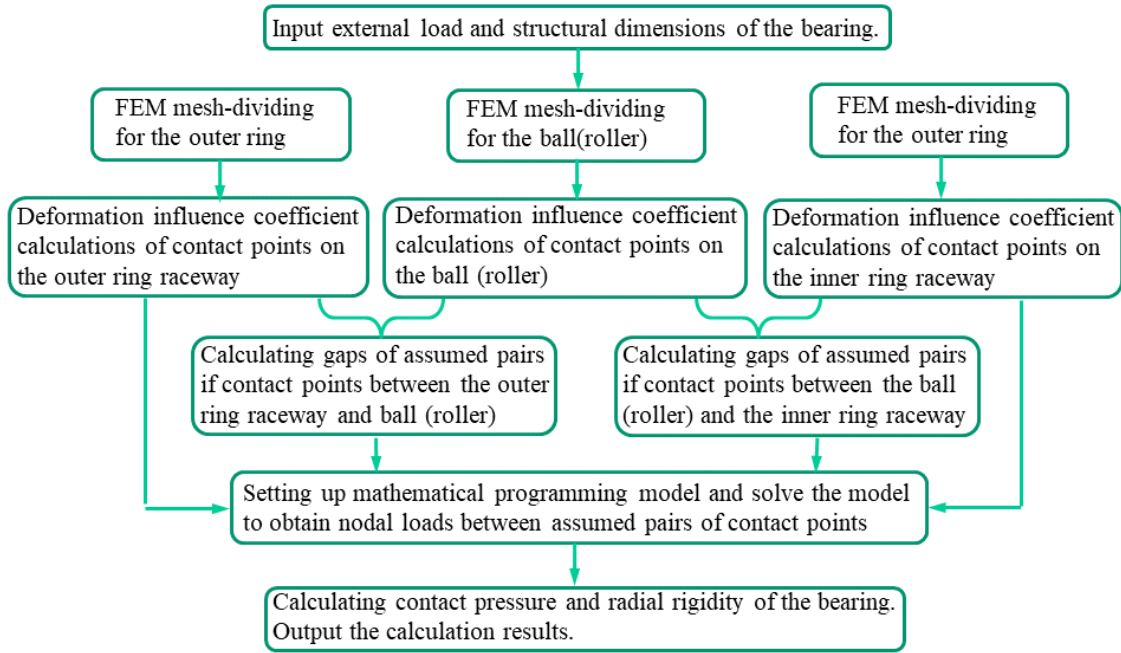


Fig. 8 Flowchart of software development for bearing contact analysis

## 5. Calculation results and discussions

### 5.1 Contact pressure distribution

Firstly, loaded bearing contact analysis is conducted for the deep groove ball bearing as shown in Fig. 1(a) with the developed software. Fig. 9(a) and 9(b) are calculated contact pressure distributed on the ball surfaces. Fig. 9(a) is a contour map of the contact pressure distribution between the ball and the outer ring raceway. Fig. 9(b) is a contour map of the contact pressure distribution between the ball and the inner ring raceway. The external load  $P$  is 7kN when the analysis is conducted. From Fig. 9, it is found that the contact pressure on the ball surface is calculated to be a beautiful elliptical distribution. The maximum contact pressure point is located at the centre of the contact area. Results in Fig. 9 are more reasonable than the ones obtained by SolidWorks and the reference [22] as given in Fig. 2 and Fig. 4(a). It is also found that the maximum contact pressure on the upper part of contact areas (the contact of the ball with the outer ring raceway) is a little smaller than the one on the lower part of contact areas (the contact of the ball with the inner ring raceway). This is because radius of curvature of the inner ring raceway is smaller than that of the outer ring raceway. Smaller radius of curvature of the contact surfaces shall bring greater contact pressure based on Hertz theory.

The maximum contact pressure of the ball bearing is also calculated according to Hertz theory. Fig. 10 is a comparison of the maximum contact pressure between the developed software and Hertz theory. In Fig. 10, abscissas are the radial load  $P$  applied on the bearing and the ordinates are the maximum contact pressure on the ball surface. Fig. 10(a) is the maximum contact pressure between the ball and inner ring raceway. Fig. 10(b) is the one between the ball and outer ring raceway. Fig. 10(a) indicates that the maximum contact pressure obtained by the developed

software (illustrated with “FEM”) is totally smaller than the one obtained by Hertz theory. Fig. 10(b) indicates that the maximum contact pressure obtained by the developed software is totally greater than the one obtained by Hertz theory. Different methods can be thought to be the reason to result in different results. As it is stated above, Hertz theory cannot consider of the total structural deformation of the ball, inner and outer ring while the developed software can consider the total structural deformation of the bearing.

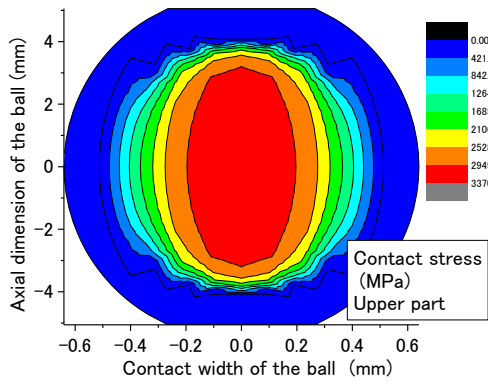
Secondly, loaded bearing contact analysis is conducted for the cylindrical roller bearing as shown in Fig. 1(b) with the developed software. Fig. 11(a) and 11(b) are calculated contact pressure distributed on the roller surface when the roller is not crowned. Fig. 11(a) is the contact pressure between the roller and the outer ring raceway. Fig. 11(b) is the contact pressure between the roller and the inner ring raceway. The external load  $P$  is 4kN when this contact analysis is conducted. From Fig. 11, it is found that contact pressure on the roller surface is calculated to be uniform distribution along the axis of the roller except for two end areas of the roller. It is also found that the edge-loads are calculated beautifully on the two end areas. By considering the fact that it is still a difficult thing at the present situation to analyse edge-loads correctly using some commercial software, it is a technical progress to be able to analyse edge-loads of an uncrowned roller bearing using the developed software. By comparing Fig. 11 with Fig. 4(b), it is also found that the developed software can calculate more reasonable results than the method introduced in the reference [22].

Loaded bearing contact analysis is also conducted for the roller bearing with crowning. Fig. 12(a) and (b) are imagines of the roller before and after crowned using Johson-Gohar curve [21] as given in Eq. (20). The crowning quantity of the roller can be considered in the gap  $\varepsilon_k$  of the pair of contact points. Calculation results for the crowned roller bearing are given in Fig. 13. Fig. 13(a) is the contact pressure distribution between the crowned roller and the outer ring raceway. Fig. 13(b) is the contact pressure distribution between the crowned roller and the inner ring raceway. From Fig. 13, it is found that the edge-loads disappeared on the two end areas of the roller and contact pressure becomes uniform distribution longitudinally in comparison with Fig. 11. It is also found that the maximum contact pressures are reduced about 17% and 21% when the roller is crowned by comparing Fig. 13(a) with Fig. 11(a) and Fig. 13(b) with Fig. 11(b). The results in Fig. 13 indicate that Johson-Gohar curve is a very nice curve for crowning of the roller bearings. It can reduce edge-loads and bring the roller bearing a uniform contact pressure distribution very well.

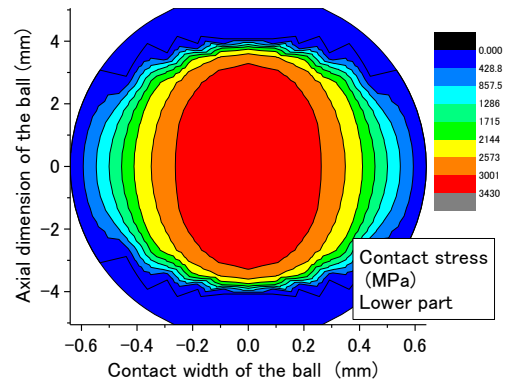
$$q(x) = \frac{2P}{\pi l E'} \ln \frac{1}{1 - (1 - 0.3033b/a)(2x/l)^2} \quad (20)$$

Where,  $l$  is effective contact length of the roller and  $a$  is a half of  $l$ .  $b$  is a half width of the contact.  $E$  is Young's modulus and  $\nu$  is Poisson's ratio.  $E'$  is equivalent Young's modulus that can be calculated using Eq. (21).  $P$  is a radial load applied on the roller.  $x$  is used to stand for longitudinal position of a point along the axis.  $q(x)$  is used to denote the drop (quantity of crowning) at the position  $x$  in the axial direction.

$$E' = \frac{E}{1 - \nu^2} \quad (21)$$

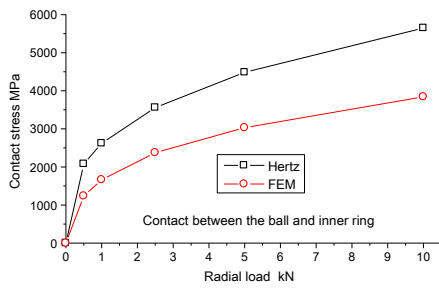


(a) The upper part of the contact domain

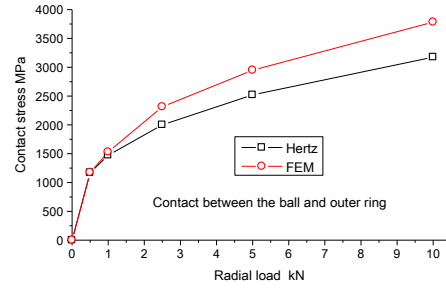


(b) The lower part of the contact domain

Fig. 9. Contour maps of contact stresses distributed on the ball surface

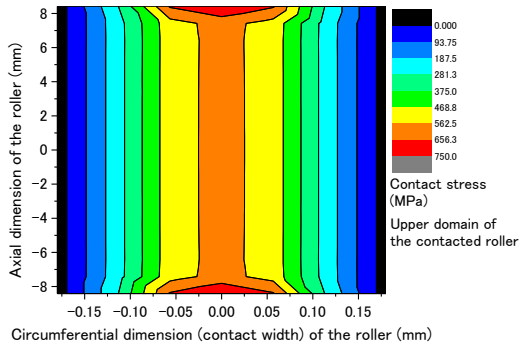


(a) Contact between the ball and inner ring

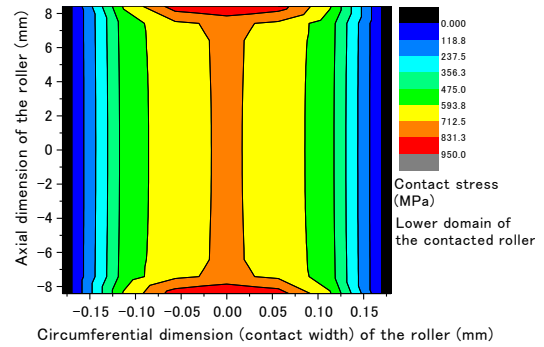


(b) Contact between the ball and outer ring

Fig. 10. Contact pressure comparison between the developed FEM software and Hertz theory



(a) The upper part of the contact domain



(b) The lower part of the contact domain

Fig. 11. Contour maps of contact stresses distributed on the roller surface

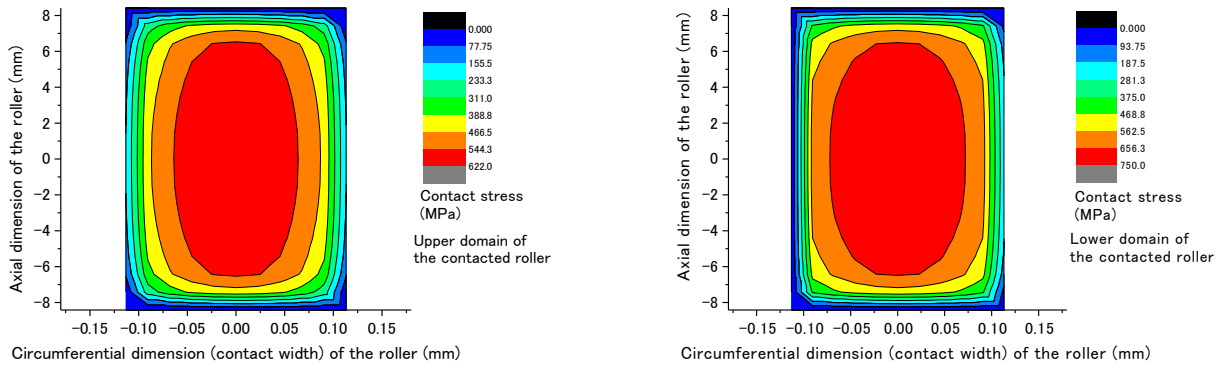


(a) The roller before crowned



(b) The roller after crowned

Fig. 12. Crowning on the two ends of the roller with Johnson-Gohar curve



(a) The upper part of the contact domain (b) The lower part of the contact domain

Fig. 13. Contour maps of contact stresses distributed on the roller surface

### 5.2 Radial rigidity of the ball bearing

In the case of the ball bearings, Hertz theory is used to calculate radial rigidity of the bearings, a comparison of the radial rigidity is made for the ball bearing between the developed software and Hertz theory in Fig. 14. From Fig. 14, it is found that the results obtained by using the developed software are greater than the ones obtained by using Hertz theory. An experimental research is scheduled to identify which method is more precise in the next research in the near future.

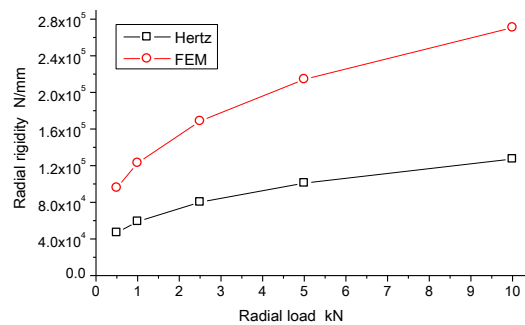


Fig. 14. Comparison of radial rigidity of the ball bearing

## 6. Applications in the future

Usually, bearing systems are affected by thermal actions, friction, lubrication cage, etc. If thermal deformation of the bearings is calculated by the finite element analysis, the proposed method can be developed to investigate the effect of the thermal actions on contact pressure distribution of the bearings in the future. Also, if the contact areas are divided very finely, unevenness of the contact surfaces can be considered precisely with the proposed method. At this case, the proposed method can be developed to investigate the effect of friction on contact pressure distribution of the bearing systems. The effect of lubrication cage of the bearings on contact rigidity and pressure of the bearings can be investigated precisely also with the proposed method. This investigation shall be conducted in the further research of the author.

## 7. Conclusions

A mathematical model and numeric method are presented in this paper to conduct contact analysis of rolling bearings based on the principle of the mathematical programming method. Three-dimensional, finite element method is introduced to calculate deformation influence coefficients and gaps of the assumed pairs of contact points between contact surfaces. Special software is developed to realize the procedures of the contact analysis. With the help of the special software, loaded bearing contact analyses are conducted for a deep groove ball bearing and a cylindrical roller bearing.

In the case of the ball bearing, it is found that calculated contact pressure on the ball surfaces is correct elliptical distribution (usually called contact ellipse). This result is more reasonable than the results obtained by commercial software SolidWorks and other researchers.

In the case of the roller bearing, it is found that edge-loads (non-Hertz contact that cannot be analyzed with Hertz theory) on the roller surface are analyzed when the roller is not crowned. It is also found that the edge-loads disappear and contact pressure on the roller surface becomes uniform distribution when the roller is crowned with Johnson-Gohar curve. The maximum contact pressure is reduced 21% when the roller is crowned with Johnson-Gohar curve.

Since the most important features (contact ellipse and edge-loads) of the bearing contacts are analyzed successfully by the developed software and these results cannot be obtained simply by general methods, the mathematical model and numeric method presented in this paper are of practical meaning in engineering design and the developed software can be used as a tool for contact strength and rigidity calculations of the rolling bearings.

An experimental research is scheduled to confirm the reliability of the method and software presented in this paper in the next research in the near future.

## Acknowledgment

NSK Foundation for the Advancement of Mechatronics is appreciated for funding this research. Mr. Ryuichi SONEZAKI, a student who graduated from Machine Design Lab in Shimane University, is also appreciated for conducting contact analysis of the ball and roller bearings with SolidWorks software under the direction of the author.

## References

- [1] Tedric A. Harris, Michael N. Kotzalas, *Essential Concept of Bearing Technology: Rolling Bearing Analysis*, Fifth Edition, CRC Press, 2007.
- [2] Tedric A. Harris, Michael N. Kotzalas, *Advanced Concepts of Bearing Technology: Rolling Bearing Analysis*, Fifth Edition, CRC Press, 2007.
- [3] S. Kamamoto, K. Fujimoto. and T. Yamamoto, Research on crowning profile to obtain maximum load carrying capacity for roller bearings, *KOYO Engineering Journal English Edition* 159 (2001) 47-52.
- [4] H. Nagatani, A new resolution to contact problem of roller bearings (in Japanese), *The Tribology* 6 (346) (2016) 44-46.
- [5] H. Zhao, Analysis of load distributions within solid and hollow roller bearings, *Trans. ASME, J. Tribology* 120 (1) (1998) 134-139.
- [6] H. Wang, S. Dai, Study on contact finite element simulation of the high-angular contact thrust ball bearing, *Computer simulation* 1 (2013) 1-70.
- [7] Z. Qi, G. Wang, Z. Zhang, Contact analysis of deep groove ball bearings in multibody systems, *Multibody system dynamics* 33 (2) (2015) 115-141.
- [8] J. Zhang, B. Fang, Y. Zhu, J. Hong, A comparative study and stiffness analysis of angular contact ball bearings

- under different preload mechanisms, *Mech. Mach. Theory* 115 (2017) 1-17.
- [9] V. Roda-Casanova, F. Sanchez-Marin, Contribution of the deflection of tapered roller bearings to the misalignment of the pinion in a pinion-rack transmission, *Mech. Mach. Theory* 109 (2017) 78-94.
- [10] L. Xu, Y. Yang, Y. Li, et al., Modeling and analysis of planar multibody systems containing deep groove ball bearing with clearance, *Mech. Mach. Theory* 56 (2012) 69-88.
- [11] L. Xu, Y. Li, An approach for calculating the dynamic load of deep groove ball bearing joints in planar multibody systems, *Nonlinear dynamics* 70 (3) (2012) 2145-2161.
- [12] L. Xu, Y. Yang, Modeling a non-ideal rolling ball bearing joint with localized defects in planar multibody systems, *Multibody system dynamics* 35 (4) (2015) 409-426.
- [13] J. Liu, Y. Shao, T. C. Lim, Vibration analysis of ball bearings with a localized defect applying piecewise response function, *Mech. Mach. Theory* 56 (2012) 156-169.
- [14] J. Liu, Y. Shao, Dynamic modeling for rigid rotor bearing systems with a localized defect considering additional deformations at the sharp edges, *J. Sound Vib.* 398 (2017) 84-102.
- [15] S. Singh, U. G. Köpke, C. Q. Howard, et al. Analyses of contact forces and vibration response for a defective rolling element bearing using an explicit dynamics finite element model, *J. Sound Vib.* 333 (21) (2014) 5356-5377.
- [16] Christophe Bovet, Laurent Zamponi, An approach for predicting the internal behaviour of ball bearings under high moment load, *Mech. Mach. Theory* 101 (2016) 1-22.
- [17] C. Machado, M. Guessasma, E. Bellenger, An improved 2D modeling of bearing based on DEM for predicting mechanical stresses in dynamic, *Mech. Mach. Theory* 113 (2017) 53-66.
- [18] Product catalogue of NTN Corporation.
- [19] Dassault Systemes SolidWorks Corporation, SolidWords Essentials.
- [20] R. Sonezaki, S. Li, Contact analysis and stiffness testing device design of rolling bearings, *JSME Mechanical Engineering Congress*, 2014, 1-4.
- [21] P. M. John, and R. Gohar, Roller bearings under radial and eccentric loads, *Tribology International* 14 (1981) 131-136.
- [22] Y. Guo, R. G. Parker, Stiffness matrix calculation of rolling element bearings using a finite element/contact mechanics model, *Mech. Mach. Theory* 51 (2012) 32-45.
- [23] T. Ishida and S. Li, A method for analyzing tooth load distribution and contact stress of a thin wall spur gear using FEM and a mathematical programming method (in Japanese), *Trans. JSME Series C* 63 (606) (1997) 585-591.
- [24] S. Li, T. Ishida, A method of analyzing tooth load distribution for a thin wall spur gear with assembly errors, *Trans. JSME, Series C* 63 (615) (1997) 4017-4024.
- [25] S. Li, Gear contact model and loaded tooth contact analysis of a three-dimensional, thin-rimmed gear, *ASME J. Mech. Des.* 124 (3) (2002) 511-517.
- [26] O. Wolfe, The simplex method for quadratic programming, *Econometrica* 27 (1959) 382-398.
- [27] I. Hiramoto, A. Hase, *Linear Programming Method*, Baifukan Co., LTD. Press, 1973.
- [28] G. Liu, *Structural Dynamics of the Finite Element Method* (In Chinese), National defense industry press, 1994.

